Flexural behavior of piles in high strain dynamic testing

Allani, M. & Holeyman, A.

Keywords: high strain pile tests, eccentric impact, flexural dynamic behavior

ABSTRACT: The flexural vibrations of piles during dynamic tests have to be carefully investigated since it is difficult to control the alignment of the ram mass with respect to the neutral axis of the pile. In this paper, we present two case histories of high strain dynamic pile testing where eccentric impacts were generated. First, measured dynamic signals are presented to show the different relationships between quantities measured at the pile head (force, velocity, bending moment and rotation rate). Then, flexural effects on dynamic pile capacity are determined by the Case Method to show effects of the impact eccentricity on dynamic bearing capacity.

1 INTROD UCTION

Pile design analysis is needed to verify required functions (bearing capacity, allowable settlement, installation feasibility…). There are three types of dynamic pile tests: 1) high strain dynamic test, 2) high strain kinetic test, also known as "rapid load test" (with a longer load application period than for the classical high strain test) and 3) integrity testing (short wavelength for better detection of anomalies in the pile) (Rausche et al 1985, Holeyman 1992, Goble 2000). We will focus in this paper on high strain dynamic testing where the main objective is to evaluate the dynamic and static bearing capacity of the pile. Static load testing remains the reference for checking a pile performance since it best approaches the real load in terms of duration and loading rate. Nevertheless, carrying out this kind of test takes a long time and involves a very expensive mobilization of the load and associated reaction. For these reasons dynamic loading tests (DLTs) have now been adopted by most engineering communities with the aim to improve productivity in terms of quality control and design confirmation. These objectives seem to be satisfactorily achieved as the test becomes more and more accepted as a routine procedure.

However, it is worth noting that DLTs still include some limitations even though high technology and sophisticated interpretation methods are used during measurement and for signal maching analysis. An important uncertainty or difficulty in a DLT is the complex combination of compressive, tensile and also bending forces. (those may induce higher stresses than in service conditions and may cause pile damage). They may also induce signals that may be hard to signal match assuming a purely axial condition.

Poskitt (1992), Holeyman (1992) and Charue (2004) indicate that eccentricity of the mass ram is often observed in DLTs. It is also well observed in pile driving where extreme conditions may be reached. Poskitt (1991, 1992, 1996) was among the few authors who addressed on the problem of non axial effects in pile driving. To study the misalignment problem, he studied the general theory of impacts in two dimensions using Smith's 1960 model to represent the loading rate effects. However, no conclusions were derived concerning the flexural effects on the bearing capacity.

In this paper, case histories of pile dynamic testing under eccentric impacts are presented. First we present the sites geotechnical conditions (Limelette and Tessenderlo site) and we detail the experimental procedure. Then, axial and flexural signal analyses are performed with a focus on transferred energy to the pile and ram-pile misalignment effects. Finally, pile capacity from dynamic measurements is determineted. The Case Method is used for the calculation of shaft, base and total soil resistance. Conclusions about flexural effects on bearing capacity are finally drawn.

2 GEOTECHNICAL SITES DESCRIPTION AND EXPERIMENTAL PROCEDURE

2.1 Geotechnical sites description

According to CPTs (Cone Penetration Tests), we deduced the following stratigraphy : 8 m thickness of silt layer over Brussellian sand layer at Limelette and compact sandy silt in the top 6 m over silt to clayey sand layer at Tessenderlo.

2.2 Experimental procedure and data reduction

Dynamic impacts on piles were generated by a Dynamic Loading Test Module. The system, called FondyTest, has been developed at the Department of Civil and Environmental Engineering of the 'Université Catholique de Louvain'' (UCL). It consists in a 4 tons ram mass with an adjustable drop height, and is easily transportable to the field (Fig. 1). The eccentricity of impact may also be controlled by a set of four air-actuated cushions. The actual eccentricity imposed in each blow was verified manually in the field.

A driven precast prestressed square concrete pile with a = 350 mm side and 9.5 m length was tested at the Limelette site. A continuous flight auger pile, with large hollow stem of diameter $2r$ = 600 mm and about 15.5 m long was tested at the Tessenderlo site.

Figure 2 presents the configuration of transducers for both sites with reference to pile axes, showing where four uniaxial piezoelectric accelerometers (Acc) and four strain gauges (Sg) were mounted.

From measured acceleration, one can obtain by integration the velocity and displacement at the pile head. Unfortunately, this task is not as easy as it seems because of environmental signal noise, parasitic errors and offsetting integration problems that might affect the integration process. For noise elimination, a non-causal filtering (Butterworth type, 6th order with 1.5 kHz cutoff frequency) was used and a corrective acceleration and velocity was incorporated to the real signals to eliminate integration offset and match independently measured pile penetration (set).

Both 500g (PCB353B04) and 5000g (PCB353M231) accelerometers were used in parallel. The 500g transducers provided the most reliable readings while the 5000g transducers prevented saturation of the signals in case acceletrations in excess of 500g land to be encountered (the maximum measured acceleration was 350g for the site of Limelette and 450g for the site of Tessenderlo).

Figure 1. DLTM transported to the field.

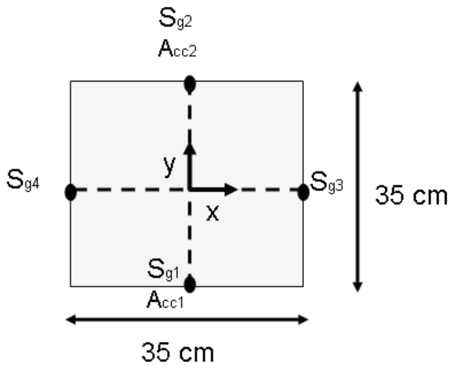

(a)

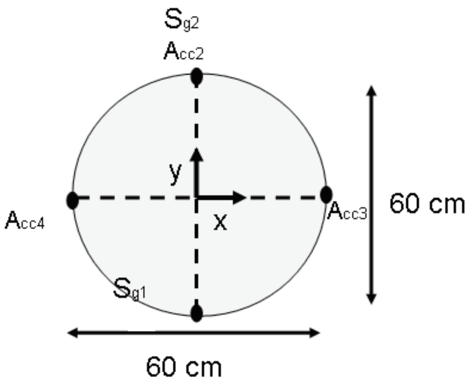

(b)

Figure 2. Sensors location at pile head for (a) Limelette and (b) Tessenderlo sites.

We also have adopted high sampling frequencies at both sites to confirm Nyquist criteria namely 20 kHz and 5 kHz for the Limelette and Tessenderlo sites respectively.

For the calculation of applied force F, we used the formula: $F = EA_p\varepsilon_{mean}$ where E is the pile young modulus, A_p is the pile cross section, and ε_{mean} is the mean measured strain where $\varepsilon_{mean}=\frac{\sum_{i=1}^{4}\varepsilon_i}{4}$ and $\varepsilon_{mean}=\frac{\sum_{i=1}^{2}\varepsilon_i}{4}$ respectively for Limelette and Tessenderlo site (as shown in Fig. 2).

Tables 1 and 2 summarize the sequential pile loading at both sites. H, e_x and e_y denote the drop height and eccentricities. Eccentric impacts in x and y directions were purposely generated at the Limelette site and only in y direction at the Tessenderlo site.

3 DYNAMIC SIGNAL ANALYSIS

3.1 *Axial Force, velocity and displacement relationships*

In the very first moments of the impact (Fig. 3), measured force and velocity times pile impedance I are superposed as functions of dimensionless time L/c where L is the pile length and $c=\sqrt{E/\rho_{pile}}$ is the bar wave propagation velocity and ρ_{pile} is the pile material density. When the peak force $F_{\max}$ is correlated to the peak velocity $V_{\max}$ (Fig. 4), the observed trend must reflect the nominal impedance of the pile I. The latter is equivalent to a dashpot factor modeling the behavior of a semi-infinite pile subjected to an imposed velocity at its head: $I=\rho_{pile}cA_p$. The impedance values obtained by such regressions (1.1 and 2.5 MN/m.s^{-1} for Limelette and Tessenderlo respectively) confirm the material values expected for the nominal properties of the impacted piles.

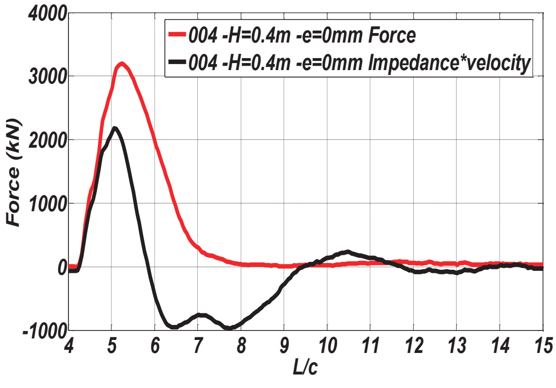

Figure 3. F and V*I signals at the Tessenderlo site.

Figure 5 presents the progression of maximum and permanent settlements versus the hammer drop height at the Limelette site. The maximum settlement curve is convex characterized by a local slope that progressively decreases with the drop height parabolic trend from the origin up to a given drop height beyond which a higher constant slope prevails. The permanent settlement curve is characterized by negligible values up to a given drop height called the 'critical height' beyond which maximum and permanent settlements tend to progress as parallel curves, separated by a constant "rebound".

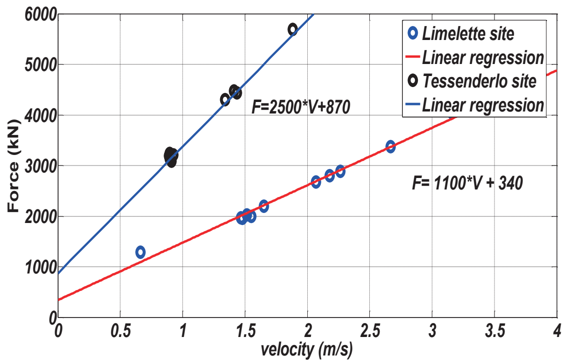

Figure 4. F_{max}-V_{max} Regression (Limelette and Tessenderlo).

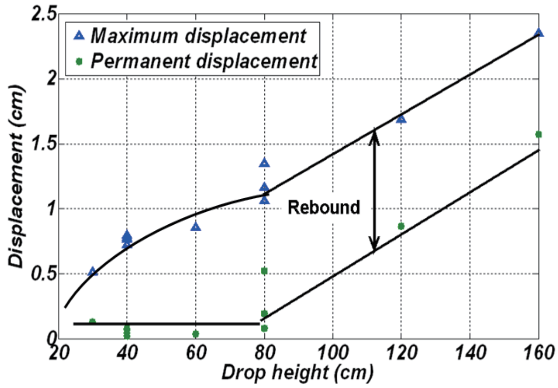

Figure 5. Permanent and maximum settlement versus drop height at the Limelette site.

3.2 *Energy analysis*

The axial energy transmitted to the pile can be calculated by integrating over time the product of force and velocity signals. The so called 'Enthru' corresponds to the peak value reaching by this integration carried until the end of impact tf:

$$Enthru=\max(\int_0^{t_f}F(t)V(t)dt) \tag{1}$$

This term reflects the performance of the system which can be compared to the hammer potential energy (M_HgH). It can be concluded (Fig. 6) that the net energy transferred to the pile amounts to approximately 80% of the hammer potential energy.

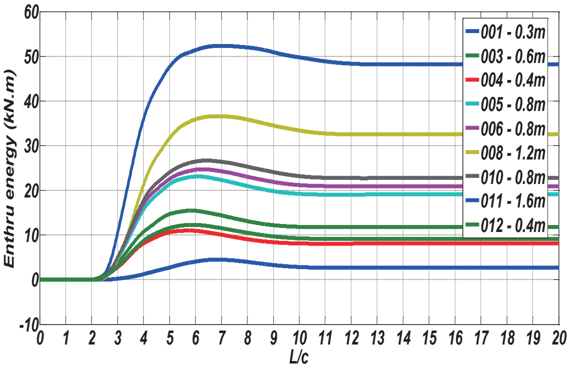

Figure 6. "Enthru" energy for the Limelette site.

The bending moment M_x (M_y) about the x-(y-) direction for both sites was calculated based on diametrically opposed measured strains (ε_1 and ε_2) on the pile head section. Bernoulli assumptions used for classical beam bending theory lead to $M = \frac{Ea^3}{12}(\varepsilon_2 - \varepsilon_1)$ and $M = \frac{E.\pi.r^3}{8}(\varepsilon_2 - \varepsilon_1)$ for square and circular cross sections, respectively. The calculation of the angular velocity $\dot{\theta}$ is calculated based on opposed measured pile head vertical velocity v_1 and v_2 as $\dot{\theta} = \frac{v_1 - v_2}{a}$. By analogy with the axial analysis, we estimate the flexural energy transmitted to the pile using the relation:

$$Enthru_{flex} = \int_0^{t_f} M(t)\dot{\theta}(t)dt \qquad (2)$$

where, M is the bending moment at the pile head and $\dot{\theta}$ is the pile head cross section angular velocity or rate of tilt.

The bending moment M_x (M_y) about the x-(y-) direction for both sites was calculated based on diametrically opposed measured strains ($\square_1$ and $\square_2$) on the pile head section. Bernoulli assumptions used for classical beam bending theory lead to $M = \frac{Ea^3}{12}(\varepsilon_2 - \varepsilon_1)$ and $M = \frac{E.\pi.r^3}{8}(\varepsilon_2 - \varepsilon_1)$ for square and circular cross sections, respectively.

The calculation of the angular velocity $\dot{\theta}$ is calculated based on opposed measured pile head vertical velocity v_1 and v_2 as $\dot{\theta} = \frac{v_1 - v_2}{d}$ (where d=a and d=2r for the site of Limelette and Tessenderlo respectively).

An example (impact 8) of individual strain measurements and velocity for the site of Limelette is presented respectively in 7 and 8.

According to Fig. 9, the flexural energy transmitted to the pile is about 1% the axial one. This value appears negligible but should not be discounted when assessing the potential importance of pile bending on its axial pile bearing capacity

Table 1. Summary of impacts, axial, flexural and soil resistance analysis for the Limelette site.

Impact				Axial			Flexural			Resistance		
Blow n°	H (cm)	e_x (mm)	e_y (mm)	V_{max} (m/s)	F_{max} (kN)	EMAX (kN.m)	M^y_{max} (kN.m)	$\dot{\theta}^y_{max}$ (rad/s)	E^y_{max} (kN.m)	R_f (MN)	Q_B (MN)	R_{dyn_case} (MN)
1,2	30	0	0	0.66	1.28	4.5	20.2	0.25	0.01	1.35	0.57	1.61
3	60	20	-20	1.65	2.19	15.5	53.1	0.62	0.07	1.80	1.66	2.68
4	40	20	-20	1.46	1.96	11.0	33.4	0.36	0.03	1.60	1.47	2.39
5	80	20	-20	2.06	2.67	23.1	42.0	0.42	0.05	1.84	2.34	3.01
6	80	20	-40	2.17	2.80	24.7	53.3	0.44	0.06	1.81	2.90	2.75
7,8	120	18	-32	2.66	3.36	36.6	113.0	1.10	0.16	1.85	3.98	2.85
9,10	80	22	-31	2.26	2.88	26.7	85.3	1.09	0.14	1.78	3.27	2.62
11	160	22	-31	3.16	4.04	52.3	123.2	1.90	0.15	1.91	5.37	3.04
12	40	2	-3	1.51	2.02	12.3	41.7	0.58	0.03	1.60	1.68	2.29
13	40	2	-40	1.55	1.99	12.3	42.6	0.51	0.02	1.59	1.70	2.30
14	40	3	-34	1.47	1.95	11.9	37.2	0.56	0.04	1.60	1.59	2.28

Table 2. Summary of impacts, axial, flexural and soil resistance analysis for the Tessenderlo site.

Impact			Axial			Flexural	Resistance		
Blow n°	H (cm)	e_y (mm)	V_{max} (m/s)	F_{max} (kN)	E_{MAX} (kN.m)	M^y_{max} (kN.m)	R_f (MN)	Q_B (MN)	R_{dyn_case} (MN)
1	70	0	1.34	4.29	17.0	38.3	3.09	3.24	6.22
2	110	0	1.88	5.69	3.0	38.2	3.70	4.60	8.14
3	40	0	0.89	3.19	9.8	37.7	2.42	2.14	4.62
4	40	37	0.89	3.13	9.7	-53.0	2.35	2.12	4.64
5	70	37	1.43	4.43	19.7	-61.7	3.02	3.44	6.61
6	40	62	0.91	3.08	9.9	-91.7	2.21	2.15	4.63
7	40	-37	0.92	3.21	10.6	89.2	2.41	2.15	4.81
8	70	-37	1.41	4.47	20.1	114.7	3.15	3.42	6.65
9	40	-55	0.89	3.24	10.4	119.9	2.44	2.15	4.71

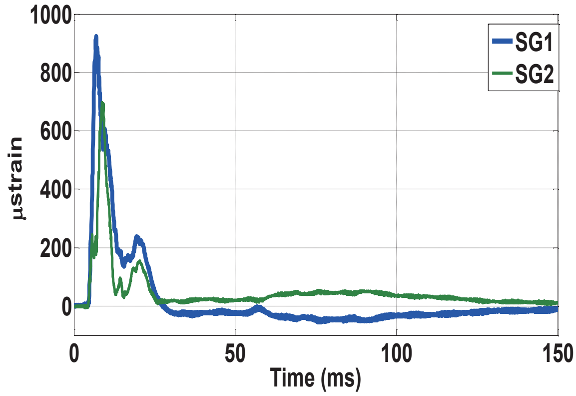

Figure 7. Strain gages measurement for impact 8 in Limelette site.

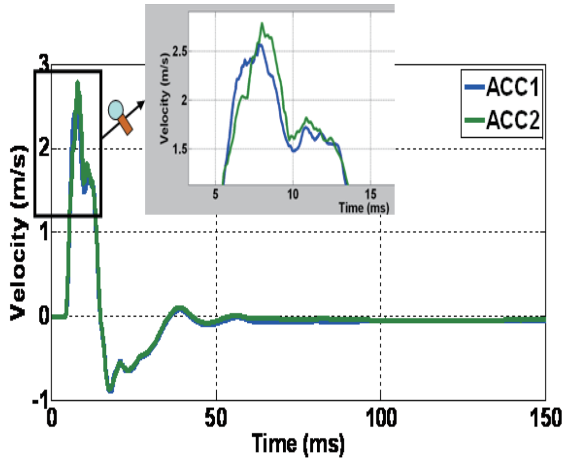

Figure 8. Velocity measurement for impact 8 in Limelette site.

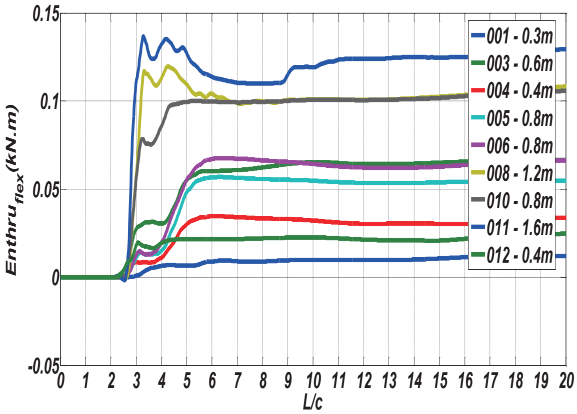

Figure 9. 'Enthruflex' traces for Limelette site.

4 DYNAMIC PILE CAPACITY DERTERMINATION

As explained is Section 3.1, pile impedance represents the proportionality between force and velocity at the impacted head of a free semi-infinite pile, i.e. in the absence of soil interaction. However, soil resistance influences upward and downward force and velocity waves in the pile (Fig. 10). The Case Method (Rausche et al 1985) is based on the difference between signals of a free pile and those of the real situation. Assuming complete mobilization of shaft and base soil resistance, the Case Method signal processing can lead to the evaluation of total resistance under high strain dynamic pile testing. The Case resistance hence postulates that all soil resistance (shaft and base) is mobilized. Validity of that assumption, especially for base modeling is discussed in Holeyman (1992) and Charue (2004). Figure 8 shows the path of a short incident wave and its interactions with the soil at depth z^* and at the pile toe at depth L.

Since the reflected upward compressive wave is related to the mobilized skin friction R_f, this latter can be evaluated as:

$$Q_f(z^*) = \int_0^{z^*=ct} R_f = 2F^{\uparrow} = F - IV \qquad (3)$$

Where $F^{\uparrow}$ is the upward force.
For the pile base, the following expression can give some indication about the toe resistance:

$$Q_B = \frac{1}{2}[F(t_B^+) + IV(t_B^+)] - \frac{1}{2}[F(t_B^+ + \frac{2L}{c}) - IV(t_B^+ + \frac{2L}{c})] \qquad (4)$$

where t_B^+ is the time selected to obtain the maximum value of Q_B within the interval: $2L/c < t_B^+ < 4L/c$.
The Case Method leads to a combination of shaft and base dynamic resistance to evaluate the total soil resistance:

$$R_{dyn\_case} = \frac{1}{2}[F(t^+) + F(t^+ + \frac{2L}{c})] + \frac{I}{2}[V(t^+) - V(t^+ + \frac{2L}{c})] \qquad (5)$$

where , time t^+ is picked as to correspond to peak velocity $V_{\max}$ (Rausche 1985, Holeyman 1992).
Total, base, and shaft soil resistance of Limelette and Tessenderlo piles are also presented in Tables 1 and 2 respectively.

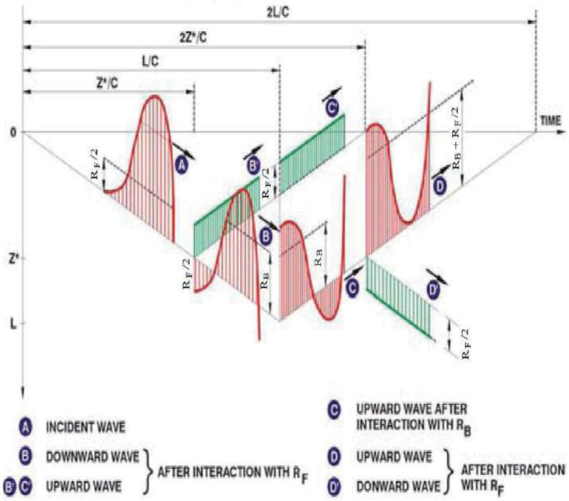

Figure 10. Sets of waves in dynamically loaded pile (Holeyman, 1992).

It was concluded that it seems reasonable to choose time t^+ at the time when first peak velocity occurs since soil Case dynamic resistance achieves a maximum value at that time. It was further confirmed that higher energy impacts mobilize more of the ultimately available soil resistance.

The effects of eccentricity on the dynamic Case soil resistance are not significant for low impacts and low eccentricities (No significant changes between eccentric and non eccentric impact for all the impact of 40cm height for both sites). For Limelette site, the only compassion that could be made is for 80cm height impact. Unfortunately, no centric impact was made and low differences of eccentricity were applied so no trend on the bearing capacity was deduced. However, an increase in the total dynamic soil resistance can be noted under eccentric impacts for Tessenderlo site for the 0.7 m drop height (about 400kN increase). In the authors opinion, the coupling effects of lateral pile vibration is noted for high impacts (so that axial soil resistance is fully mobilized) together with large eccentricity.

Basing on these conclusions, it would be interesting in future work to investigate the range of hammer drops versus eccentricity where axial soil resistance increases.

5 AXIAL AND FLEXURAL RESPONSE

Several numerical models (TNOWAVE, CAPWAP, SIMBAT, NUSUM-UCL…) approach pile/soil interaction by a computer simulation with a view to reproduce measured force and velocity signals. Either the force or the velocity (or a combination of signals like the downward force wave) can be imposed as a stimulus boundary condition of the model (Charue 2004). The measured axial force-velocity trace (Fig. 11) can also be used to visually assess the quality of matching procedure (Charue, 2004).

The same reasoning may also be applied to the flexural mode. Allani and Holeyman (2010) elaborated a back calculation scheme to assess lateral soil stiffness and damping under steady state lateral pile loading. Curves of experimental bending moment versus pile head angular velocity (Fig. 12) allow one to graphically monitor the corresponding optimization procedure curve which is presently undergoing development.

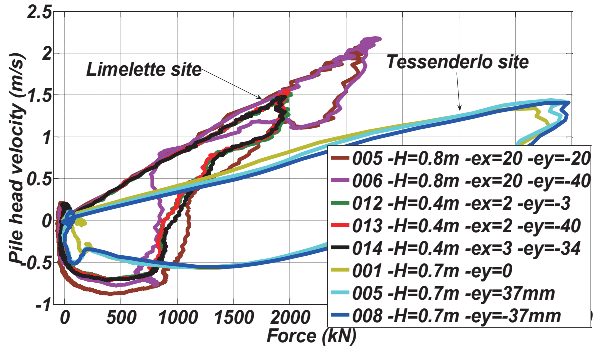

Figure 11. Measured axial load-velocity curves for Limelette and Tessenderlo sites.

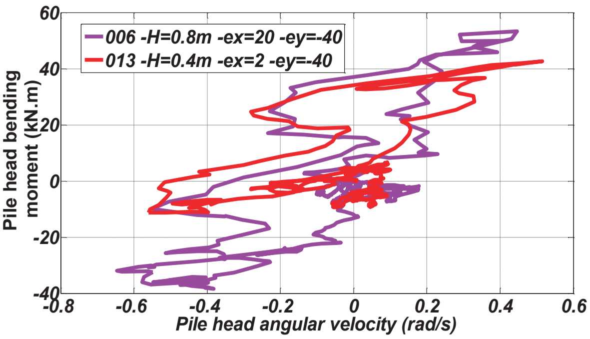

Figure 12. Measured $M^y - \dot{\theta}^y$ curves at the Limelette site.

Case resistance analysis.

6 CONCLUSION

Two case histories of axial and flexural signal analysis resulting from high strain dynamic pile tests have been presented. Data show that dynamic moments can be generated during impact. Although high eccentricity was applied during impacts, transferred flexural energy was noted to be very small compared to the axially transferred one. However, an increase of the Case Method dynamic soil resistance was observed under eccentric impacts at the Tessenderlo site. By analogy to the current axial analysis, a flexural response representation has been suggested at the pile head as a reference to deduce lateral soil stiffness and damping through a back-calculation matching algorithm.

We conclude that a specific formulation should be used to model the eccentric impact together with a numerical model for coupling the analysis between axial and lateral pile responses (Allani & Holeyman 2012).

REFERENCES

Allani. M and Holeyman A. (2010). Non axial effects in dynamic pile testing: Pile vibration analysis using Timoshenko beam theory. Geotechnical Engineering 20, View of Young European Geotechnical Engineers, Brno, 158-163.

Allani M and Holeyman A (2010). Signal analysis of axial and flexural behavior in high strain dynamic pile testing. Proceedings of the 2nd International conference on Geotechnical Engineering, Hammamet, Tunisia, 477-486.

Allani M and Holeyman A (2012). Numerical developments of lateral pile-soil behavior in pile driving. Submitted to the 9th International Conference on testing and Design Methods for Deep Foundation. IS-Kanazawa. Japan.

Charue N (2004), Loading rate effects on pile load-displacement behaviour derived from back calculation analysis of two load testing procedure. Thesis dissertation (Université Catholique de Louvain, UCL, Belgium).

Holeyman A.E (1992), Keynote lecture: Technology of pile dynamics, Proceedings of the fourth international conference on the application of stress wave theory to piles, 195-215. A.A Balkema, Rotterdam, Netherlands.

Poskitt T.J. (1991). Energy loses in pile driving due to soil rate effects and hammer misalignment. Proceedings Institution of Civil Engineers; 823:851-91.

Poskitt T.J. (1992). Keynote lecture: problems of reconciling stress wave measurements with theory. Proceedings of the fourth international conference on the application of stress wave theory to piles, 495-507. A.A Balkema, Rotterdam, Netherlands.

Poskitt T.J. (1996). The deflection of piles during driving. Géotechnique, 46 (2), 235 –243

Rausche F, Goble G.G, Likins G.E. (1985) Dynamic determination of pile capacity, Journal of geotechnical Engineering, 11, 367-383.

Smith, E.A.L. (1960). Pile driving analysis by the wave equation. Journal of soil mechanics and foundation division.(ASCE). 6(4), 35-61.

Van Alboom G, and Whenham V. (2003). Soil investigation campaign at Limelette (Belgium) Results. In Proceeding of the Symposium on screw piles in sand. Design and recent development Swets and Zeitlinger, Eds.